Probabilistic approach for predicting periodic orbits in piecewise affine differential models

Madalena Chaves, Etienne Farcot, Jean-Luc Gouzé

This is a preliminary version of the article published as:
M. Chaves, E. Farcot and J.-L. Gouzé, Bull. Math. Biology, 75(6), pp. 967-987, 2013.

Probabilistic approach for predicting periodic orbits in piecewise affine differential models*

Madalena Chaves† Etienne Farcot‡ Jean-Luc Gouzé§

Abstract

Piecewise affine models provide a qualitative description of the dynamics of a system, and are often used to study genetic regulatory networks. The state space of a piecewise affine system is partitioned into hyperrectangles which can be represented as nodes in a directed graph, so that the system's trajectories follow a path in a transition graph. This paper proposes and compares two definitions of transition probability between two nodes A and B of the graph, based on the volume of the initial conditions on the hyperrectangle A whose trajectories cross to B. The parameters of the system can thus be compared to the observed transitions between two hyperrectangles. This property may become useful to identify sets of parameters for which the system yields a desired periodic orbit with a high probability, or to predict the most likely periodic orbit given a set of parameters, as illustrated by a gene regulatory system composed of two intertwined negative loops.

1 Introduction

The class of piecewise affine (PWA) differential models provides a qualitative description of the dynamical behavior of a system [11, 17] in polytopes and is commonly used to describe biological regulatory networks, where the data available is often of a qualitative form [13, 1]. The PWA systems to be considered here are characterized by a set of piecewise linear differential equations with continuous solutions. The state space of the PWA system is partitioned into finitely many hyperrectangles, also called *domains*, and its trajectories evolve by switching between these domains [16, 3]. The dynamics of these systems can also be described by a discrete transition graph: each domain is represented by a discrete state, and each trajectory is represented by a sequence of transitions between discrete states, so that the full qualitative dynamical behaviour is represented by a directed transition graph. In general, there may be multiple transitions from the same domain, and in this case the transition graph provides no information on which transition is "more likely".

In this study, we explore the idea of associating a *probability* of transition to each of the edges in the discrete transition graph, in terms of the parameters of the PWA model (see also [15], for a first approach). A probabilistic approach was also suggested in [20], but for a simpler class of PWA systems, those where each variable has one single threshold value and the degradation rates are equal for all variables. In this case, the partition of the state space consists of a grid with only two intervals for each variable, the trajectories are straight lines, and a simple formula can be deduced. A different probabilistic approach has been developed in [21] to describe perturbations in the transition graph of synchronous Boolean networks, in the form of Markov chains. Although our approach can be ultimately also described by a Markov chain, our goal is not to study the properties of such systems, but rather to introduce a framework that relates the discrete transition graph to the parameters and properties of the differential PWA systems (with a view to parameter estimation, for instance). Other probabilistic approaches in the literature use experimental data to construct a graph of interactions between families of related genes, and thus obtain full networks of interactions [19, 10].

We propose and analyze two alternative definitions of transition probability based on the volume of initial conditions whose trajectories will switch from domain A to domain B. One of the definitions depends only on the current state while the other involves some memory of the trajectory of the system (Section 3). If the transition probabilities between domains can be experimentally measured, this concept can be applied to estimate some

*This work was supported in part by the INRIA-INSERM project ColAge and by ANR project GeMCo (ANR 2010 BLAN 0201 01).
†BIOCORE, INRIA, 2004 Route des Lucioles, BP 93, 06902 Sophia Antipolis, France,madalena.chaves@inria.fr
‡Virtual Plants, INRIA, Avenue Agropolis, 34398 Montpellier, France. etienne.farcot@inria.fr
§BIOCORE, INRIA, 2004 Route des Lucioles, BP 93, 06902 Sophia Antipolis, France, jean-luc.gouze@inria.fr

of the model's parameters. Another application is the analysis of the asymptotic behaviour of systems whose directed transition graph exhibits several possible transition cycles. This raises the (typically difficult) question of whether the corresponding piecewise continuous system admits a periodic orbit [6]. The definitions of transition probability will be used to provide an approximative answer to this question (Section 5). Other problems to be discussed include finding sets of parameters that lead to a given periodic trajectory (Section 4), and to control the system from one periodic trajectory to another, by appropriately changing the inputs/parameters (Section 6). These problems are illustrated by application to a reduced model of a regulatory network involving Nuclear Factor κB and its own inhibitor, a system which has the potential to exhibit several forms of oscillatory behaviour.

2 Piecewise affine differential models

A class of piecewise affine (PWA) differential models was first introduced by Glass and co-authors [13], motivated by genetic regulatory networks. Various mathematical aspects of these systems have recently been studied in detail [16, 3], including the definition of solutions across thresholds, sliding mode solutions, and the stability of steady states. The existence of periodic orbits for these systems has been studied, for instance, in [14, 6, 9], as well as some control problems [1, 17, 8, 4]. We briefly recall useful facts for our problem.

2.1 The general model

Let $x \in \mathbb{R}^n_{\geq 0}$, $f : \mathbb{R}^n_{\geq 0} \to \mathbb{R}^n_{\geq 0}$ a piecewise constant function (f is constant over domains, as described below) and $\Gamma = \mathrm{diag}(\gamma_1, \ldots, \gamma_n)$ a diagonal matrix with $\gamma_i > 0$, and consider the n-dimensional system,

$$\dot{x} = f(x) - \Gamma x. \tag{1}$$

The function f represents the interactions between the various components of the system, for instance, the activation or inhibition effects between different proteins (see the example in Section 4), and is usually defined as a combination (sum of products) of Heaviside (or *step*) functions. An activation ($x_i \to x_j$) is represented by a positive step function,

$$s^+(x_i, \theta_i) = \begin{cases} 0, & x < \theta_i \\ 1, & x > \theta_i \end{cases}$$

and an inhibition ($x_i \dashv x_j$) by a negative step function, $s^-(x_i, \theta_i) = 1 - s^+(x_i, \theta_i)$. The positive step function can be interpreted as follows: protein x_i will strongly influence the production of another protein x_j once it reaches an appropriate concentration θ_i; below this threshold concentration, x_i does not influence x_j. (Similary for s^-.) To characterize the function f, we will assume that each variable x_i has p_i *thresholds*:

$$0 < \theta_i^1 < \cdots < \theta_i^{p_i} < M_i := \theta_i^{p_i+1}, \tag{2}$$

where $M_i = \max\{\frac{f_i(x)}{\gamma_i} : x \in \mathbb{R}^n_{\geq 0}\}$. These thresholds partition the state space into *regular domains* in which the vector fields are given by a linear function. To label these domains, we will use the notation:

$$B^{k_1 k_2 \cdots k_n} : \quad k_i \in \{0, 1, \ldots, p_i\}, \quad \theta_i^{k_i} < x_i < \theta_i^{k_i+1},$$

with $\theta_i^0 := 0$. So, for $n = 3$ and $(p_1, p_2, p_3) = (1, 2, 2)$, B^{102} denotes the cube $x_1 \in (\theta_1^1, M_1)$, $x_2 \in (0, \theta_2^1)$, and $x_3 \in (\theta_3^2, M_3)$. The segments defining the borders of the regular domains are called *switching domains*, since a group of variables is at a threshold value, and are denoted by:

$$D^{l_1 \cdots l_n} : \quad l_i = \theta_i^{k_i}, i \in I_s, \quad l_j = k_j, j \notin I_s,$$

where I_s is the set of indices corresponding to those variables at a threshold. In this paper, the function f takes a constant value in each regular domain:

$$f(x) = f^{k_1 k_2 \cdots k_n}, \in \mathbb{R}^n_{\geq 0}$$

so that an expression for the system

$$\dot{x} = f^{k_1 k_2 \cdots k_n} - \Gamma x \tag{3}$$

can be explicitly written for each regular domain. Observe that, in each regulatory domain, the system of equations is decoupled and each variable is governed by an equation of the form $\dot{x}_i = a_i - \gamma_i x_i$, with $a_i = f_i^{k_1 k_2 \cdots k_n}$ a non-negative constant. The solutions are thus increasing or decreasing exponentials. The point $\phi^{k_1 k_2 \cdots k_n} = (f_1^{k_1 k_2 \cdots k_n}/\gamma_1, \ldots, f_n^{k_1 k_2 \cdots k_n}/\gamma_n)$ is called the *focal point* of the domain $B^{k_1 k_2 \cdots k_n}$. If $\phi^{k_1 k_2 \cdots k_n} \in B^{k_1 k_2 \cdots k_n}$, then the focal point is an equilibrium of the system in the classical sense. The solutions of the system are thus continuous functions, and can be formed by concatenating the segments from each domain. The crossing between two regular domains (the function f is not defined at switching domains) can be defined in a natural way if the vector fields are not opposing on each side of the boundary [3]. Otherwise, solutions can still be defined, in the sense of Filippov [16]. For simplicity, throughout this paper we will assume that no sliding mode solutions (i.e. $x_i(t) \equiv \theta_i$ for some time interval) are present in the systems to be studied. In fact, we will consider systems that contain no focal points on the switching domains, and have only "transparent" boundaries, that is, adjacent domains have vector fields which can be naturally continued.

2.2 Transition graph

From (3), for a trajectory starting in a given domain $B^{k_1 \cdots k_n}$ there are two generic possibilities: (i) if the domain contains its focal point $\phi^{k_1 k_2 \cdots k_n}$, then this is actually a locally asymptotically stable equilibrium point and the trajectory will remain in $B^{k_1 \cdots k_n}$ for all times; (ii) if the focal point $\phi^{k_1 k_2 \cdots k_n} \notin B^{k_1 \cdots k_n}$, then the trajectory will leave $B^{k_1 \cdots k_n}$ at some instant. In case (ii), the trajectory will exit from the domain as soon as one of the variables reaches a threshold. Suppose that variable k_l is the first to reach a threshold; then we say that there is a transition

$$B^{k_1 \cdots k_n} \;\rightarrow\; B^{k_1 \cdots \tilde{k}_l \cdots k_n}, \quad \tilde{k}_l \in \{k_l - 1, k_l + 1\}. \tag{4}$$

A third possibility is that of a trajectory passing through a vertex of the domain, in which case two or more variables switch simultaneously. These are, however, non-generic situations as they correspond to a very specific choice of initial conditions (often called a separatrix, see equation (6) below for an example). We will not consider transitions that involve more than one switching variable. In this way, a *discrete transition graph* can be associated to a PWA system (1), where the set of vertices is the family of domains $B^{k_1 \cdots k_n}$, for all k_i, and the edges are given by (4). Let

$$\mathcal{N}(B^{k_1 \cdots k_n}) = \{B^{k_1 \cdots \tilde{k}_l \cdots k_n} : \exists \text{ trajectory evolving from } B^{k_1 \cdots k_n} \text{ to } B^{k_1 \cdots \tilde{k}_l \cdots k_n}\}.$$

The elements of $\mathcal{N}(B^{k_1 \cdots k_n})$ are called the *successors of* $B^{k_1 \cdots k_n}$.

Definition 2.1 Consider system (1) and let $V = \{B^{k_1 \cdots k_n} : k_i \in \{0, 1, \ldots, p_i\}\}$ be a set of vertices and $E = \{B^{k_1 \cdots k_n} \rightarrow B^{k_1 \cdots \tilde{k}_l \cdots k_n} : B^{k_1 \cdots \tilde{k}_l \cdots k_n} \in \mathcal{N}(B^{k_1 \cdots k_n})\}$ a set of edges. The pair (V, E) is called the *transition graph* of system (1).

To simplify notation, the elements in V will be denoted B^a, $a \in \{1, \ldots, |V|\}$, where $|V|$ is the number of elements in V. Often, B^r will denote a reference domain and B^i one of its adjacent domains, obtained by switching the variable x_i. Throughout this paper, we will consider that each edge in the transition graph can only connect two vertices that differ on a single index k_l , i.e., only one discrete variable is allowed to change at each transition. Note that, in this graph, any domain B may have at most n successors. This graph was first suggested by L. Glass, when he initially introduced piecewise linear models of gene networks [12], and later the notion was also used in situations with multiple thresholds by E.H. Snoussi [22]. More details on its construction and main properties can also be found in [7, 5]. For an example of a transition graph see Fig. 5.

In a transition graph (V, E), a *path* is a sequence of vertices in V which are connected by edges in E. A closed path will be called a transition cycle (see also [6]):

Definition 2.2 A set of L distinct vertices in V which are connected by edges in E and visited in a sequence

$$B^1 \rightarrow \cdots \rightarrow B^L \rightarrow B^1$$

such that the last transition returns to the first vertex is called a *transition cycle of length L*.

Note that any periodic solution of (1) will generate a transition cycle of the graph (V,E), but the existence of a transition cycle does not imply the existence of a periodic orbit. More generally, every trajectory of a PWA system (excluding those with simultaneous switching of several variables) follows a path in the transition graph, but the converse is false: there can be paths in the transition graph that are not followed by any trajectory of the underlying PWA system. As a stronger result, it can also happen that, given a state transition graph, for all PWA systems whose parameters are leading to this graph there are paths that are not followed by any trajectory [7]. In this sense, a PWA system can be seen as discrete, multi-valued system with additional constraints on the allowed transitions, that are imposed by the underlying continuous state space of PWA systems. This connects them with the much-studied asynchronous multivalued logical models [23], whose transition structure is identical to a discrete transition graph of the form above, often with additional constraints which are expressed in terms of relative speeds of the different elements in the system. This similarity only holds at the qualitative level of the transition graph, and it can also happen that, even if a path is followed by continuous trajectories of a PWA system the dynamical nature of the two systems differ. The most typical situation is when a transition cycle, which is a periodic evolution, corresponds to damped oscillations in the PWA system, and thus to a stable steady state. The general question of predicting the evolution of a PWA system based on its discrete transition graph and its parameters is still largely open, although some particular cases have been considered [22, 7, 5]. The difficulty of this problem is in fact one motivation of the approach undertaken in this paper: if one cannot predict exactly the asymptotic dynamics, it can still be valuable to provide probabilistic estimates.

In this paper, we will assume that there are at most two successors for each region:

Hypothesis 1 (H1) For all $B^r \in V$, card$(\mathscr{N}(B^r))\leq 2$, so there exist at most two coordinates x_i, x_j such that the transitions $B^r \to B^i$ or $B^r \to B^j$ (where $B^i = B^{k_1 \cdots \tilde{k}_i \cdots k_n}$) are contained in the set E.

In this case, a trajectory starting from any initial condition in B^r will either cross to B^i or B^j, dividing B^r into two subregions. This assumption is made in order to obtain manageable computations, but we are able to consider interesting and nontrivial problems (see the examples below) when different transition cycles intersect. Remark that, although only two transitions are allowed from each domain, *there are no constraints on the dimension n of the system*.

3 Transition probabilities in the graph

The transition graph contains information on the possible pathways for a trajectory, but it provides no indication on whether a given pathway is more likely than another. The goal of the present analysis is to relate dynamical aspects determined by the systems's parameters (here, activity thresholds, synthesis and degradation rates) to *probabilities* of transition between two state space hyperrectangles, $P(B^r \to B^i)$.

Under hypothesis H1, the transition from B^r to B^i or B^j can be studied in the 2D plane (x_i, x_j). Following Section 2, there are three cases to analyze:

(i) B^r contains its focal point. Then, any trajectory starting in B^r remains in B^r so $P(B^r \to B^i) = 0$, for all $i \neq r$;

(ii) B^r does not contain its focal point and there is only one possible transition, to some B^i. Then, trivially, $P(B^r \to B^i) = 1$;

(iii) B^r does not contain its focal point and there are two possible transitions, to B^i and B^j. Two definitions for $P(B^r \to B^i)$ will be suggested below.

In case (iii), assume that θ_i^r and θ_j^r are the thresholds that may be crossed, and consider also the two closest thresholds for each variable:

$$\theta_i^{r-1} < \theta_i^r < \theta_i^{r+1}, \quad \theta_j^{r-1} < \theta_j^r < \theta_j^{r+1}.$$

The locus of the initial points from which a trajectory ends in (θ_i^r, θ_j^r) is a separatrix curve dividing the region B^r into two subsets from which transitions are possible to B^i or B^j. This separatrix can be exactly computed from the equations of the system in B^r:

$$\dot{x}_i = f_i^r - \gamma_i x_i, \tag{5}$$

whose solutions are of the form

$$x_i(t) = (x_{i0} - M_i)e^{-\gamma_i t} + M_i$$

with $M_i = \frac{f_i^r}{\gamma_i}$ (similarly for x_j). The separatrix is given by setting $x_i(t) = \theta_i^r$ and $x_j(t) = \theta_j^r$, and solving both equalities with respect to t, that is:

$$\left(\frac{\theta_i^r - M_i}{x_{i0} - M_i}\right)^{1/\gamma_i} = e^{-t} = \left(\frac{\theta_j^r - M_j}{x_{j0} - M_j}\right)^{1/\gamma_j},$$

and now solving this equation for x_{j0} as a function of x_{i0}:

$$\sigma(x_i) = M_j + (\theta_j^r - M_j)\left(\frac{x_i - M_i}{\theta_i^r - M_i}\right)^{\frac{\gamma_j}{\gamma_i}}. \tag{6}$$

To relate kinetic parameters to probabilities of transition, one idea is to compare the *volumes* of the two subregions of B^r above and below the separatrix [15]: that is, the probability of crossing from B^r to B^i would be given by the fraction of the volume of B^r corresponding to initial conditions that evolve to B^i. This has a natural biological interpretation as follows. Suppose a given experiment is repeated N times, always with initial conditions in B^r (that is, initial concentrations in the intervals defined by B^r) and one counts the number of times N_i that the system evolves to B^i. Then the quotient N_i/N can be viewed as the probability that trajectories of system (5) switch from B^r to B^i.

However, a careful look at Fig. 1 shows that the history of the trajectory may lead to more precise values. Indeed, in Fig. 1 a), if the trajectory enters the box B^r from the region $x_i < \theta_i^{r+H_i}$, $\theta_j^r < x_j < \theta_j^{r+H_j}$, then it will always proceed to B^j, by uniqueness of solutions inside B^r. In the next subsections, we propose and compare two possible definitions for transition probability, with or without *memory* of the previous transition.

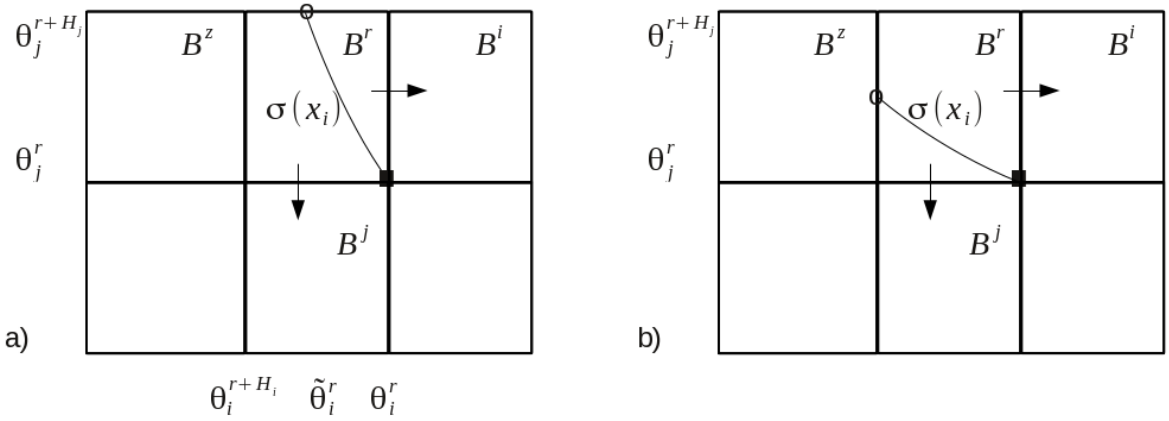

Figure 1: General case: inside the initial box B^r, there are two possibilities for the starting point of curve σ, depending on the parameters. The starting point is labeled by an open circle. The ending point (black square) is always (θ_i^r, θ_j^r). a) the trajectories of the whole region B^z cross to region B^j through B^r; b) the trajectories can cross from B^z to either B^i or B^j.

3.1 One-step transition probabilities

We will first introduce a *memoryless* definition of transition probability which depends only on the starting (or reference) box. For a general domain B^r, let (θ_i^r, θ_j^r) denote the ending point of the separatrix, and define

$$H_i = \begin{cases} 1, & x_i > \theta_i^r \\ -1, & x_i < \theta_i^r \end{cases}$$

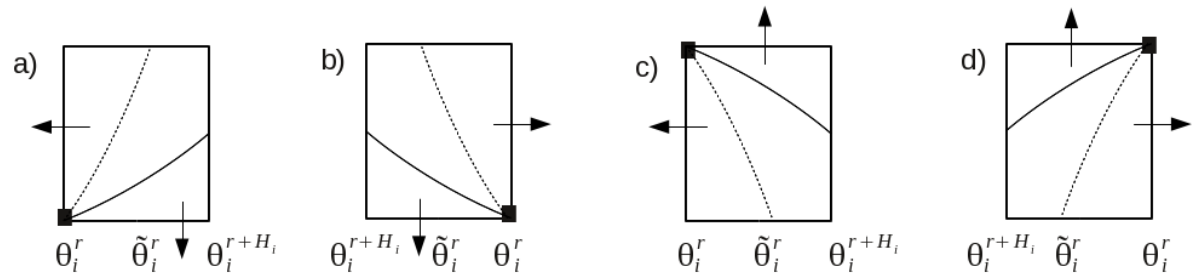

Figure 2: The four different configurations for two exits (black arrows) out of a domain B^r. Horizontal (resp., vertical) coordinate is x_i (resp., x_j). The separatrix curves are represented in solid black if $\theta_i^s = \theta_i^{r+H_i}$ and dashed if $\theta_i^s = \tilde{\theta}_i$. Their endpoints coincide at (θ_i^r, θ_j^r). In configurations a) and b), the area under the separatrix represents a transition $B^r \to B^j$ while for configurations c) and d), the area under the separatrix represents a transition $B^r \to B^i$.

Then, one can see that a point (x_i, x_j) belongs to B^r iff

$$\min\{\theta_i^r, \theta_i^{r+H_i}\} < x_i < \max\{\theta_i^r, \theta_i^{r+H_i}\}, \;\; \min\{\theta_j^r, \theta_j^{r+H_j}\} < x_j < \max\{\theta_j^r, \theta_j^{r+H_j}\}.$$

As illustrated by Fig. 1, there are two possibilities for the starting point of the separatrix in B^r, depending on whether the curve hits a vertical or horizontal threshold first. Let $\tilde{\theta}_i$ denote the coordinate x_i of the separatrix's starting point, which is defined by:

$$\sigma(\tilde{\theta}_i) = \theta_j^{r+H_j} \;\; \Leftrightarrow \;\; \tilde{\theta}_i = M_i + (\theta_i^r - M_i)\left(\frac{\theta_j^{r+H_j} - M_j}{\theta_j^r - M_j}\right)^{\frac{\gamma_i}{\gamma_j}}.$$

The starting point of the separatrix is thus given by

$$(\theta_i^s, \sigma(\theta_i^s)) \;\; \text{with} \;\; \theta_i^s = \begin{cases} \theta_i^{r+H_i}, & \tilde{\theta}_i \notin [\min\{\theta_i^r, \theta_i^{r+H_i}\}, \max\{\theta_i^r, \theta_i^{r+H_i}\}] \\ \tilde{\theta}_i, & \tilde{\theta}_i \in [\min\{\theta_i^r, \theta_i^{r+H_i}\}, \max\{\theta_i^r, \theta_i^{r+H_i}\}]. \end{cases} \tag{7}$$

In the panel (a) of Fig. 1 $\theta_i^s = \tilde{\theta}_i$, while in panel (b) $\theta_i^s = \theta_i^{r+H_i}$.

Hypothesis H1 implies that there are only four configurations to be analyzed, which are depicted in Fig. 2. The area corresponding to initial conditions in the box B^r which are below the separatrix curve can be calculated as follows.

Lemma 3.1 Given a domain B^r from which transitions are possible to the domains B^i and B^j, consider the corresponding separatrix curve (6), with endpoint (θ_i^r, θ_j^r) and starting point $(\theta_i^s, \sigma(\theta_i^s))$ as in (7). Define

$$\alpha = \min\{\theta_i^r, \theta_i^s\}, \quad \beta = \max\{\theta_i^r, \theta_i^s\}.$$

The area of the box B^r under the curve (6) is given by:

$$A_\sigma = \int_\alpha^\beta \sigma(x)dx - \min\{\theta_j^r, \theta_j^{r+H_j}\}(\beta - \alpha) + \frac{1}{2}(1 + H_j)\left|\theta_j^r - \theta_j^{r+H_j}\right|\left|\theta_i^s - \theta_i^{r+H_i}\right|$$

where the integral $\int_\alpha^\beta \sigma(x)dx$ is given by

$$M_j(\beta - \alpha) + \frac{\gamma_i}{\gamma_i + \gamma_j}(\theta_j^r - M_j)(\theta_i^r - M_i) \times \left(\left(\frac{\beta - M_i}{\theta_i^r - M_i}\right)^{1+\frac{\gamma_j}{\gamma_i}} - \left(\frac{\alpha - M_i}{\theta_i^r - M_i}\right)^{1+\frac{\gamma_j}{\gamma_i}}\right).$$

■

The term $\min\{\theta_j^r, \theta_j^{r+H_j}\}(\beta-\alpha)$ represents the area of the boxes just below B^r, which are counted in the integration (it is naturally zero if there is no box below B^r, i.e. $\min\{\theta_j^r, \theta_j^{r+H_j}\}=0$). If $H_j>0$ and $\theta_i^s=\tilde{\theta}_r$, the term $\left|\theta_j^r-\theta_j^{r+H_j}\right|\left|\theta_i^s-\theta_i^{r+H_i}\right|$ reflects the area in B^r which is not covered by the integral between α and β (see a) and b) in Fig. 2).

Furthermore, the area A_σ reflects the basin of attraction of B^r from where transitions are possible to B^i (if $H_j>0$) or B^j (if $H_j<0$), which leads to the following definition. From hypothesis H1, we have immediately that the two probabilities of transition add up to one.

Definition 3.2 Consider a trajectory $\varphi(t;x_0)$ that starts in a domain B^r, and assume that there are two possible transitions from B^r, to B^i (horizontal coordinate) or B^j (vertical coordinate). The *1-step transition probability from B^r to B^j* is:

$$P_{rj}^{\text{one}}=\begin{cases}\dfrac{A_\sigma}{\left|\theta_i^r-\theta_i^{r+H_i}\right|\left|\theta_j^r-\theta_j^{r+H_j}\right|}, & \text{if } H_j>0\\ 1-\dfrac{A_\sigma}{\left|\theta_i^r-\theta_i^{r+H_i}\right|\left|\theta_j^r-\theta_j^{r+H_j}\right|}, & \text{if } H_j<0.\end{cases} \tag{8}$$

3.2 Two-step transition probabilities

An alternative definition is now suggested, which involves some memory of the path followed by the trajectory along the transition graph. This is motived by the case depicted in Fig. 1: in panel (a), it is clear that any trajectory crossing from B^z to B^r cannot cross over to B^i (by uniqueness of solutions in B^r), so one may say that the transition probability from B^r to B^j, *knowing that the trajectory comes from B^z*, is in fact 1.

To introduce this alternative definition, observe that the transition to the domain B^r from some other domain B^z corresponds to crossing a threshold of some variable x_k. So, one of two cases must hold:

(i) $k=i$ or $k=j$;

(ii) $k\neq i,j$.

In case (i), the two consecutive transitions take place in the *2-dimensional plane* (x_i,x_j) (this is indeed the case depicted in Fig. 1, where $k=i$), and the boundary between B^z and B^r, ∂_{zr}, is a segment. Assuming, without loss of generality, that $k=i$, we will say that the probability of a path $B^z\to B^r\to B^j$ is proportional to the length of ∂_{zr} that lies below the starting point of the separatrix $x_{j0}=\sigma(x_{i0})$.

In case (ii), the transitions can be studied in the *3-dimensional space* (x_i,x_j,x_k) (see Fig. 3), and the boundary between B^z and B^r is a planar surface with $x_k=\theta_k^r$. Since there are only two possible directions to exit B^r, the separatrix has the same expression for any value of the variable $x_k\in[\min\{\theta_k^r,\theta_k^{r+H_k}\},\max\{\theta_k^r,\theta_k^{r+H_k}\}]$ and defines a surface that divides B^r in two parts (bold lines in Fig. 3). In this case, the transition from B^r to B^j depends on the point of the plane $x_k=\theta_k^r$ where the trajectory crosses from B^z to B^r, and so the probability of a path $B^z\to B^r\to B^j$ is proportional to the *surface* of the boundary between B^z and B^r that lies below $\sigma(x_i)$ (shaded area in Fig. 3). This is the same as in Definition 3.2.

Recall the notation $B^r=B^{k_1\cdots k_n}$, and $B^j=B^{k_1\cdots\tilde{k}_j\cdots k_n}$, where $\tilde{k}_j\in\{k_j-1,k_j+1\}$.

Definition 3.3 Consider a trajectory $\varphi(t;x_0)$ that crosses from a domain B^z to B^r, corresponding to a threshold of variable x_k, and assume that there are two possible transitions from B^r, to B^i or B^j. The *two-step transition probability between B^r and B^j, given B^z* is defined as:

$$P_{rj}^{\text{two}}(z)=\begin{cases}P_{rj}^{\text{one}}, & \text{if } k\notin\{i,j\}\\ \dfrac{\min\left\{\left|\theta_j^r-\sigma(\theta_i^{r+H_i})\right|,\left|\theta_j^r-\theta_j^{r+H_j}\right|\right\}}{\left|\theta_j^r-\theta_j^{r+H_j}\right|}, & \text{if } k=i\end{cases} \tag{9}$$

If $k\notin\{i,j\}$, assume that the space is oriented according to (x_i,x_j,x_k), and if $k=i$ it is oriented (x_i,x_j). In either case: $P_{ri}^{\text{two}}(z)+P_{rj}^{\text{two}}(z)=1$.

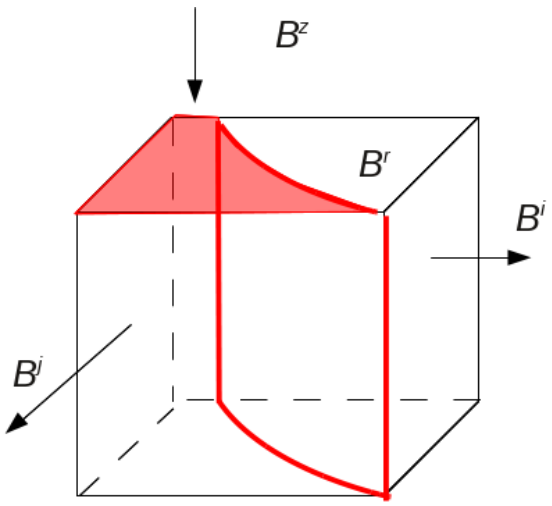

Figure 3: Transition from B^z to B^r, and then to B^i or B^j in a 3-dimensional plane. The bold lines represent the surface generated by $\sigma(x_i)$. The shaded area represents the transition probability from B^r to B^j, knowing that the trajectory comes from B^z.

4 Application: periodic orbits in biological regulatory networks

To illustrate the usefulness of the concept of transition probability, we will study the dynamics of a 3-dimensional system composed of two intertwined negative feedback loops (Fig. 4). It is inspired by a reduced model of the

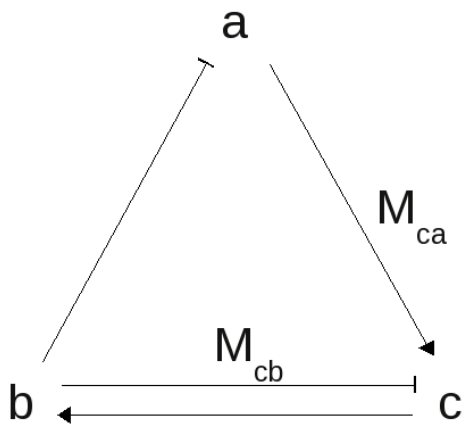

Figure 4: Network consisting of two negative loops.

NF-κB /IκB system (see [24] for more details), where a =[NF-κB]$_{cytoplasm}$, b =[IκB], and c =[NF-κB]$_{nucleus}$. Oscillatory behaviour has been experimentally observed for this system [18]. The variables a and c have one threshold each (resp., θ_a and θ_c) while b has two thresholds since it influences two other variables (θ_{ba} and θ_{bc}). Variable c has two incoming arrows which combine to generate two distinct activity levels: M_{ca} and M_{cb}.

The model can be written in the piecewise constant framework as:

$$\begin{aligned} \dot{a} &= \gamma_a(s^-(b,\theta_{ba}) - a) \\ \dot{b} &= \gamma_b(s^+(c,\theta_c) - b) \\ \dot{c} &= \gamma_c(M_{ca}s^+(a,\theta_a) + M_{cb}s^-(b,\theta_{bc}) - c), \end{aligned} \tag{10}$$

where we have assumed, to reduce the number of parameters, that the maximal values of a and b have been normalized to 1, and that c has been normalized to θ_c, so $\theta_c = 1$. We will assume that the parameters satisfy the

inequalities

$$0 < \theta_a < 1, \quad 0 < \theta_{ba} < \theta_{bc} < 1,$$
$$0 < M_{cb} < 1 < M_{ca}. \tag{11}$$

Under these conditions, variable a has two regions (corresponding to one threshold quantity) and b, c both have three regions. So the state space can be divided into 18 regions, which can be labelled B^{ijk}, where $i \in \{0,1\}$ and $j,k \in \{0,1,2\}$.

We have chosen parameters satisfying conditions (11) because they imply that system (10) has only simple transitions and no equilibria in either the classical or Filippov senses. The corresponding transition graph has several transition cycles, as shown in Fig. 5. Observe that B^{002}, B^{110}, B^{111}, B^{120}, and B^{121} are transient domains, that is, once a trajectory leaves one of these domains, it will never return to it. The asymptotic behaviour is thus represented by the bold arrows in Fig. 5. The transition diagram has five distinct transition cycles in the sense of Definition 2.2: one cycle of length 6 ($c6$) and two cycles each of length 8 ($c8a$, $c8b$) and 10 ($c10a$, $c10b$). These are characterized below in Definition 5.1. In particular, note that each of the non-transient domains represented in Fig. 5 has *at most two successors*, the only domains that admit two successors being B^{112}, B^{012}, and B^{021}. The method described in Section 3 can thus be applied to the asymptotic dynamics of system (10), since hypothesis H1 is satisfied.

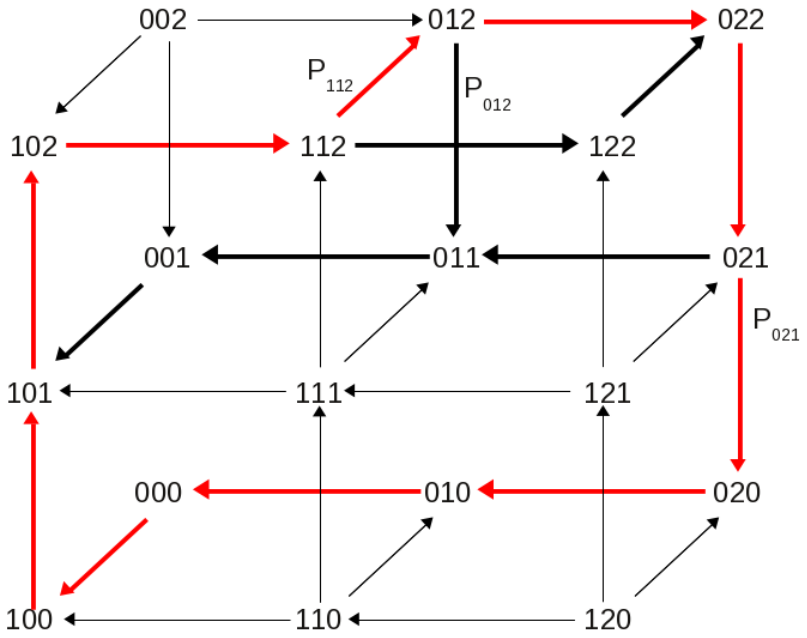

Figure 5: Transition diagram for system (10). The bold edges represent the asymptotic behaviour of the system, where five distinct cycles (of lengths 6, 8 or 10 transitions) are possible.

The dynamics of system (10) under conditions (11) is thus expected to exhibit oscillatory solutions following one of the five transition cycles. However, there is no general method to predict whether every transition cycle gives rise to a periodic orbit (for some specific set of parameters) or, conversely, which sets of parameters lead to a given periodic orbit. In the remainder of this paper, we will propose a method that gives a probabilistic answer to these two questions.

4.1 Computing transition probabilities

The probabilities of transition associated with each arrow in the graph of Fig. 5 can be computed according to Definitions 3.2 and 3.3. For the states where only one transition is possible the probability is, of course, equal to

1. Define the following new parameters, in terms of relative distances between thresholds:

$$A=\frac{1}{\theta_a},\quad B=\frac{1-\theta_{ba}}{1-\theta_{bc}},\quad C=\frac{M_{ca}}{1-M_{cb}},\quad D=\frac{1}{\theta_{bc}},\quad E=\frac{1}{M_{cb}}, \tag{12}$$

and the ratios between degradation rates:

$$g_{ab}=\frac{\gamma_a}{\gamma_b},\quad g_{bc}=\frac{\gamma_b}{\gamma_c}.$$

Note that all $A,B,C,D,E>1$, by assumption on the parameters. For simplicity of notation, we will abbreviate: $P_{112}\equiv P_{112\to 012}$, $P_{012}\equiv P_{012\to 011}$, and $P_{021}\equiv P_{021\to 020}$.

Computation of the probabilities of transition yields:

Proposition 4.1 The one-step probabilities of transition associated with the graph of Fig. 5 are given by:

$$P_{112}^{\text{one}}=\begin{cases}\frac{B}{B-1}+\frac{1}{1+\frac{1}{g_{ab}}}\frac{1-A^{1+\frac{1}{g_{ab}}}}{(A-1)(B-1)}, & \text{if } \theta_a^s=1\\ \frac{1}{(A-1)(B-1)}\left[B(B^{g_{ab}}-1)-\frac{B^{g_{ab}+1}-1}{1+\frac{1}{g_{ab}}}\right], & \text{if } \theta_a^s=\frac{B^{g_{ab}}}{A}\end{cases}$$

$$P_{021}^{\text{one}}=\begin{cases}\frac{1}{E-1}\left[\frac{1}{1+\frac{1}{g_{bc}}}\frac{D^{1+\frac{1}{g_{bc}}}-1}{D-1}-1\right], & \text{if } \theta_b^s=1\\ 1-\frac{1}{(D-1)(E-1)}\left[E(E^{g_{bc}}-1)-\frac{E^{g_{bc}+1}-1}{1+\frac{1}{g_{bc}}}\right], & \text{if } \theta_b^s=\frac{E^{g_{bc}}}{D}\end{cases}$$

$$P_{012}^{\text{one}}=\begin{cases}\frac{1}{C-1}\left[\frac{1}{1+\frac{1}{g_{bc}}}\frac{B^{1+\frac{1}{g_{bc}}}-1}{B-1}-1\right], & \text{if } \theta_b^s=\theta_{ba}\\ 1-\frac{1}{(C-1)(B-1)}\left[C(C^{g_{bc}}-1)-\frac{C^{g_{bc}+1}-1}{1+\frac{1}{g_{bc}}}\right], & \text{if } \theta_b^s=1+C^{g_{bc}}\left(\frac{1}{D}-1\right).\end{cases}$$

∎

Proposition 4.2 The two-step probabilities of transition associated with the graph of Fig. 5 are given by:

$$\begin{aligned}P_{112}^{\text{two}}&=\frac{A\theta_a^s-1}{A-1},\quad \theta_a^s=\min\left\{1,\frac{B^{g_{ab}}}{A}\right\};\\ P_{021}^{\text{two}}&=\frac{D(1-\theta_b^s)}{D-1},\quad \theta_b^s=\min\left\{1,\frac{E^{g_{bc}}}{D}\right\};\\ P_{012}^{\text{two}}&=P_{012}^{\text{one}}.\end{aligned}$$

Proof: For the case $102\to 112\to 122,012$ (configuration as in Fig. 2 c): the domain B^{112} corresponds to $a\in(\theta_a,1)$, $b\in(\theta_{ba},\theta_{bc})$ and $c\in(1,M_{ca}+M_{cb})$. The coordinate c is constant throughout these regions, and the coordinate b strictly decreases along $102\to 112\to 012$, so we will take $x_k=a$, $x_i=a$, and $x_j=b$, with $\theta_i^r=\theta_a$, $H_i=1$ and $\theta_j^r=\theta_{bc}$, $H_j=-1$. The result follows from (9), with $k=i$. The values of the constants can be obtained by looking at the equations in box B^{112}: $M_i=0$, $M_j=1$, $\theta_i^{r+H_i}=1$, $\theta_j^{r+H_j}=\theta_{ba}$.

For the case $022\to 021\to 011,020$ (configuration as in Fig. 2 a): the domain B^{021} corresponds to $a\in(0,\theta_a)$, $b\in(\theta_{bc},1)$ and $c\in(M_{cb},1)$. The coordinate a is constant throughout these regions, so we will take $x_k=b$, $x_i=b$, and $x_j=c$, with $\theta_i^r=\theta_{bc}$, $H_i=1$ and $\theta_j^r=M_{bc}$, $H_j=-1$. The result follows from (9), with $k=i$. The values of the constants can be obtained by looking at the equations in box B^{021}: $M_i=0$, $M_j=1$, $\theta_i^{r+H_i}=1$, $\theta_j^{r+H_j}=1$.

Finally, the case $112\to 012\to 022,011$ (configuration as in Fig. 2 b): the domain B^{012} corresponds to $a\in(0,\theta_a)$, $b\in(\theta_{ba},\theta_{bc})$ and $c\in(1,M_{ca}+M_{cb})$. In the two transitions from B^{012} coordinates b or c may change, and in the previous transition coordinate a changes. This means that we are in the case $k\notin\{i,j\}$, with $x_k=a$, $x_i=b$, and $x_j=c$. By Definition 3.3, we have $P_{012}^{\text{two}}=P_{012}^{\text{one}}$. ∎

4.2 Parameter identifiability and estimation

Propositions 4.1 and 4.2 show how the transition probabilities can be expressed in terms of the parameters of the system. This suggests a first application of the probabilities, for parameter estimation given experimental measurements of P_{rj}^{one} or P_{rj}^{two}.

In the present framework, the working hypothesis is that the transition probabilities are an output of the system, that is, they can be experimentally measured. In this example, there are only three independent probabilities: P_{112}, P_{012}, and P_{021}, so one may expect to be able to estimate at most three quantities/functions on the parameters of the system, including some of the thresholds. The independent parameters of the system are: θ_a, θ_{ba}, θ_{bc}, M_{ca}, M_{cb}, g_{ab}, and g_{bc}.

By re-arranging the expressions in Propositions 4.1 or 4.2, one may obtain expressions for the parameters that satisfy any given triple of probabilities. To simplify, we will do this only for Proposition 4.2. It will be useful to note that the transition from B^{012} satisfies the configuration depicted in Fig. 2 b), which means that:

$$\text{if } \tilde{\theta}_b < \theta_{ba} \text{ then } \theta_b^s = \theta_{ba} \quad \text{and} \quad \text{if } \tilde{\theta}_b > \theta_{ba} \text{ then } \theta_b^s = \tilde{\theta}_b.$$

In particular, $\theta_b^s = \max\{\theta_{ba}, \tilde{\theta}_b\}$ and

$$\theta_b^s = \theta_{ba} \;\Leftrightarrow\; C^{g_{bc}} > B.$$

Using this observation, we can obtain the following characterization.

Proposition 4.3 Consider a triple of probabilities $P_{112}^{\text{two}} \in (0,1]$, $P_{021}^{\text{two}}, P_{012}^{\text{two}} \in (0,1)$. A family of parameters that satisfies Proposition 4.2 can be expressed in terms of $B, C > 1$, as given by (12), and either

$$F_1(B) > \max\left\{ B^{\frac{1}{g_{bc}}} - 1, \frac{1}{\left(\frac{B - P_{021}^{\text{two}}}{B-1}\right)^{\frac{1}{g_{bc}}} - 1} \right\} \tag{13}$$

with

$$C - 1 = F_1(B) = \frac{1}{P_{012}^{\text{two}}} \left[\frac{1}{1 + \frac{1}{g_{bc}}} \frac{B^{1+\frac{1}{g_{bc}}} - 1}{B-1} - 1 \right]$$

or

$$C^{g_{bc}} - 1 \le F_2(C) < \frac{1 - P_{021}^{\text{two}}}{\left(\frac{C}{C-1}\right)^{g_{bc}} - 1} \tag{14}$$

with

$$B - 1 = F_2(C) = \frac{1}{1 - P_{012}^{\text{two}}} \frac{1}{C-1} \left[C(C^{g_{bc}} - 1) - \frac{C^{g_{bc}+1} - 1}{1 + \frac{1}{g_{bc}}} \right]$$

For both cases (13) and (14), the other parameters satisfy:

$$\left(\frac{B-1}{B - P_{021}^{\text{two}}}\right)^{\frac{1}{g_{bc}}} < M_{cb} < \frac{C-1}{C}, \qquad M_{ca} = C(1 - M_{cb}), \tag{15}$$

and

$$\theta_a \begin{cases} = \frac{P_{112}^{\text{two}}}{P_{112}^{\text{two}} + B^{g_{ab}} - 1}, & P_{112}^{\text{two}} < 1 \\ > 1/B^{g_{ab}}, & P_{112}^{\text{two}} = 1 \end{cases} \tag{16}$$

$$\theta_{bc} \begin{cases} = \frac{1 - P_{021}^{\text{two}}}{1/M_{cb}^{g_{bc}} - P_{021}^{\text{two}}}, & P_{021}^{\text{two}} > 0 \\ > M_{cb}^{g_{bc}}, & P_{021}^{\text{two}} = 0 \end{cases} \tag{17}$$

$$\theta_{ba} = 1 - B(1 - \theta_{bc}). \tag{18}$$

Proof: First, we establish some bounds for M_{cb} in terms of B, C, and P_{021}^{two}. Inequalities (15) hold because:

$$\frac{C-1}{C} = 1 - \frac{1}{M_{ca}} + \frac{M_{cb}}{M_{ca}} > M_{cb}$$

for all $M_{cb} \in (0,1)$ (comparison of the functions x and $1+(x-1)/M_{ca}$). And also

$$\frac{1}{B-1} = \frac{1-\theta_{bc}}{\theta_{bc}-\theta_{ba}} > \frac{1-\theta_{bc}}{\theta_{bc}} = \frac{1}{\theta_{bc}} - 1 \;\Leftrightarrow\; \frac{1}{B-1} + 1 > \frac{1}{\theta_{bc}}$$

which implies

$$1 - P_{021}^{\text{two}} = \frac{\frac{1}{\theta_{bc}}\theta_b^s - 1}{\frac{1}{\theta_{bc}} - 1} > \frac{\frac{1}{\theta_{bc}}\theta_b^s - 1}{\frac{1}{B-1}}$$

Evaluate this expression at $\theta_b^s = \frac{\theta_{bc}}{M_{cb}^{g_{bc}}}$ to obtain the left hand side inequality in (15):

$$\frac{1-P_{021}^{\text{two}}}{B-1} + 1 > \frac{1}{M_{cb}^{g_{bc}}} \;\Leftrightarrow\; \left(\frac{B-1}{B-P_{021}^{\text{two}}}\right)^{\frac{1}{g_{bc}}} < M_{cb}.$$

Now, one can easily obtain inequalities (13) and (14), after some simple algebra, using (15) together with the expressions of P_{012}^{two} for $\theta_b^s = \theta_{ba}$ or $\theta_b^s = 1 + C^{g_{bc}}\left(\frac{1}{D} - 1\right)$. Finally, expressions (16) follow directly from the definitions of P_{112}^{two}, P_{021}^{two}, and B. ∎

Thus, by measuring probabilities of transition, one may first recover an interval for the ratio B and then the ratio C follows from the value of B. The values B and C define an interval for the parameter M_{cb}. The threshold θ_a can be calculated directly from P_{112}^{two} and B; the thresholds θ_{ba} and θ_{bc} can be calculated from P_{021}^{two}, B, and M_{bc}.

To visualize these conditions, we will consider in more detail the case of equal degradation rates: $g_{ab} = g_{bc} = 1$. In this case, the interval defined by (14) is nonempty. The sets of possible parameters are depicted in Fig. 6.

Corollary 4.4 Assume $g_{ab} = g_{bc} = 1$ and consider a triple of probabilities $P_{021}^{\text{two}}, P_{112}^{\text{two}} \in (0,1]$, $P_{012}^{\text{two}} \in (0,1)$. If $P_{021}^{\text{two}} = 0$, then the parameters satisfy

$$B > C > 1, \quad M_{cb} < \frac{B-1}{2P_{012}^{\text{two}} + B - 1}, \quad \theta_{bc} > M_{cb}.$$

If $0 < P_{021}^{\text{two}} < 1$, then there is a nonemtpy set of parameters only if $1 - P_{021}^{\text{two}} > 2P_{012}^{\text{two}}$ and

$$B > \frac{1}{P_{021}^{\text{two}}}, \text{ with } C = 1 + \frac{B-1}{2P_{012}^{\text{two}}}$$

and

$$\frac{B-1}{B-P_{021}^{\text{two}}} < M_{cb} < \frac{B-1}{2P_{012}^{\text{two}} + B - 1}.$$

In both cases, $M_{ca} = C(1-M_{cb})$ and θ_a, θ_{bc}, θ_{ba} are given by (16)-(18). ∎

5 Predicting the transition cycle

The transition diagram on Fig. 5 has five distinct transition cycles, as indicated at the beginning of Section 4. In this context, Propositions 4.2 and 4.3 can be used as a guide for choosing parameters that yield a system with a periodic orbit of a given length, or passing through desired domains. For instance, it is clear that setting $P_{021} = 0$ prevents a cycle of length 10. Similarly, setting $P_{112} = 1$ and choosing a large P_{012} leads to a high probability of obtaining a length 6 cycle.

To formalize the idea that the orbit of system (10) follows a given transition cycle with a certain probability, we will now assume that the system has a unique stable periodic orbit and, for each set of parameters, define a *predicted transition cycle*.

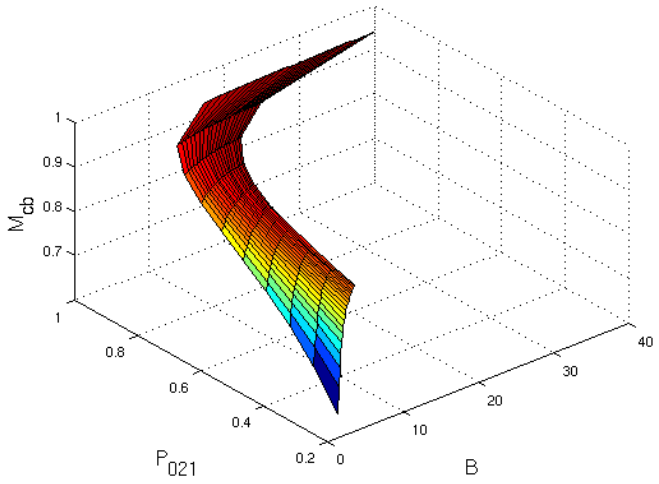

Figure 6: Range of values admitted for B and M_{cb} in terms of P_{021}^{two}, in the case of equal degradation constants. The case $P_{012}^{\text{two}} = 0.1$ is shown.

Definition 5.1 Given any set of parameters, the probability that a periodic orbit of system (10) follows each one of the transition cycles is:

$$\begin{aligned} P(c6) &= P_{112}P_{012}, \\ P(c8a) &= P_{112}(1-P_{012})(1-P_{021}), \\ P(c8b) &= (1-P_{112})(1-P_{021}), \\ P(c10a) &= P_{112}(1-P_{012})P_{021}, \\ P(c10b) &= (1-P_{112})P_{021}. \end{aligned}$$

The *predicted transition cycle* to be followed by the periodic orbit is c^{pred} such that:

$$P(c^{pred}) = \max\{P(c6), P(c8a), P(c8b), P(c10a), P(c10b)\}.$$

Note that the five probabilities add up to 1. An immediate question is whether the predicted transition cycle is a reasonable indication of the actual observed cycle. We have answered this question by performing $L = 5000$ numerical experiments as follows:

1. randomly generate a set of parameters and simulate system (10);
2. compute the probabilities $P(c)$ ($c \in \{c6, \ldots, c10b\}$) and $P(c^{pred})$ directly from the parameters;
3. observe which periodic orbit is attained by the simulated system, c^{obs} ;
4. compare c^{obs} with c^{pred}.

Similar numerical experiments were run for both the one-step and two-step models for the transition probabilities, and the results are summarized in the histogram of Fig. 7. We observed that the one-step probability model predicted the correct transition cycle on around 60% of the simulations, while the two-step model is correct up to 70%.

These simulations also show that length 8 transition cycles are the most frequent, and correspond to the cycles where the one-step transition probabilities have a poorer predictive performance (namely, for cycle $c8a$). For the other cycles, the one- and two- step probabilities appear to perform in a similar way. Recall that the probability of obtaining a $c8a$ cycle is given by $P_{112}(1-P_{012})(1-P_{021})$. The value of P_{012} is the same for both definitions of transition probability, but P_{112} and $1-P_{021}$ often take the value 1 for the two-step definition, something which can never occur for the one-step definition. This may be an explanation of the better accuracy of the two-step definition. In other words, the fact that memory can be used to rule out some exit directions appears to improve the predictive power.

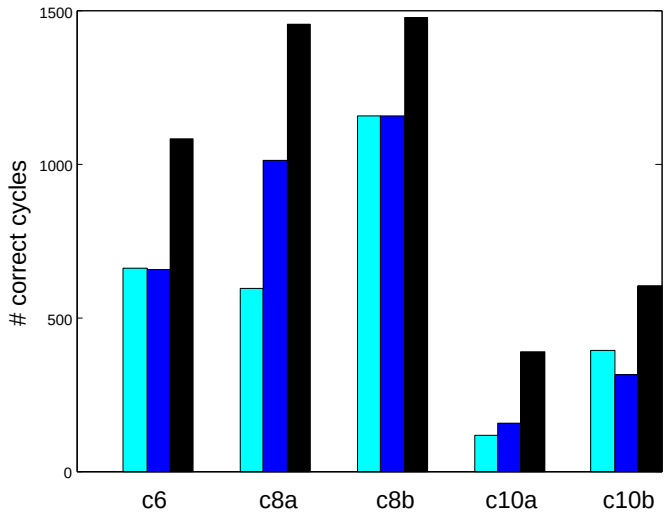

Figure 7: Histograms of the distribution of transition cycles over 5000 simulations. Black bars represent all observed cycles. Dark-grey (resp., light-grey) bars represent the correctly predicted cycles using the two-step (resp., one-step) transition probability.

6 Controlling the system to a given cycle

Another application of the previous results is to control or guide system (10) to a desired cycle, by changing only a small set of parameters. We will use Definition 5.1 in conjunction with Propositions 4.2 and 4.3 to construct a control (in the sense of finding a suitable set of parameters) that drives the system to follow a target cycle. Throughout this section, it will be assumed that the production rates M_{ca} and M_{cb} can be controlled. These can be interpreted as the "weights" of each of the negative feedback loops in the dynamics of the system: note that the system with $M_{cb} = 0$ is a single 3-dimensional negative feedback loop. This system has a unique stable periodic orbit, following cycle $c6$, as shown in [9].

Thus, in Propositions 6.1 to 6.3 below it will be assumed that θ_a, θ_{ba}, and θ_{bc} are given, and that $g_{ab} = g_{bc} = 1$, for simplicity. Under this assumption, the parameter B and the probability P_{112}^{two} are also given.

Proposition 6.1 The predicted transition cycle is of length 10 if

$$M_{cb} > \frac{2\theta_{bc}}{1+\theta_{bc}}, \quad M_{ca} > (1-M_{cb})\left(1+\frac{B-1}{2}\frac{G(M_{cb})}{\frac{1}{\theta_{bc}}-\frac{1}{M_{cb}}}\right)$$

where

$$G(M_{cb}) = \begin{cases} \max\left\{\frac{2}{\theta_{bc}}-\frac{1}{M_{cb}}-1,\ \frac{P_{112}^{\text{two}}}{1-P_{112}^{\text{two}}}\left(\frac{1}{\theta_{bc}}-1\right)\right\}, & \text{if } P_{112}^{\text{two}} < 1 \\ \frac{2}{\theta_{bc}}-\frac{1}{M_{cb}}-1, & \text{if } P_{112}^{\text{two}} = 1. \end{cases}$$

∎

The proof follows from Corollary 4.4 by requiring that $P(c10i) > P(c8i)$ and $P(c10i) > P(c6)$ $(i = a, b)$.

Proposition 6.2 Assume $P_{112}^{\text{two}} < 1$. The predicted transition cycle is of length 8 if

$$\theta_{bc} < M_{cb} < \frac{2\theta_{bc}}{1+\theta_{bc}}, \quad M_{ca} > (1-M_{cb})\left(1+\frac{B-1}{2}\frac{P_{112}^{\text{two}}}{1-P_{112}^{\text{two}}}\frac{\frac{1}{\theta_{bc}}-1}{\frac{1}{M_{cb}}-1}\right)$$

or

$$M_{cb} < \theta_{bc}, \quad M_{ca} > (1-M_{cb})\left(1+\frac{B-1}{2}\max\left\{\frac{1}{2}, \frac{P_{112}^{\text{two}}}{1-P_{112}^{\text{two}}}\right\}\right).$$

Table 1: Transition probabilities, computed according to Prop. 4.2 and Def. 5.1. The column "Nominal value" contains the data relative to the set of randomly generated parameters shown in (19). The columns "Prop. 6.3" and "Prop. 6.1" contain the new data, corresponding to parameter sets that satisfy the respective propositions.

Parameter	Nominal value	Prop. 6.3	Prop. 6.1
M_{cb}	0.6991	0.1937	0.9324
M_{ca}	3.6727	1.0064	3.6727
P^{two}_{112}	1.0	1.0	1.0
P^{two}_{021}	0.2608	0.0	0.8754
P^{two}_{012}	0.0457	0.8789	0.0096
$P(c6)$	0.0457	0.8789	0.0096
$P(c8a)$	0.7054	0.1211	0.1234
$P(c8b)$	0.0	0.0	0.0
$P(c10a)$	0.2489	0.0	0.8670
$P(c10b)$	0.0	0.0	0.0

If $P^{\text{two}}_{112} = 1$, then the predicted transition cycle is of length 8 if

$$\theta_{bc} < M_{cb} < \frac{2\theta_{bc}}{1+\theta_{bc}}, \quad M_{ca} > 1$$

or

$$M_{cb} < \theta_{bc}, \quad M_{ca} > (1-M_{cb})\left(1+\frac{1}{2}\frac{B-1}{2}\right).$$

∎

The proof is similar to that of Proposition 6.1.

Proposition 6.3 Assume $P^{\text{two}}_{112} \leq 1$. The predicted transition cycle is of length 6 if

$$M_{cb} < \theta_{bc}, \quad M_{ca} < (1-M_{cb})\left(1+\frac{B-1}{2}\min\left\{\frac{1}{2}, \frac{P^{\text{two}}_{112}}{1-P^{\text{two}}_{112}}\right\}\right).$$

∎

The proof is again similar to the previous ones, using the fact that the inequality $P(c6) > P(c8a)$ can only be satisfied if $P^{\text{two}}_{021} = 0$.

As a numerical example, one of the randomly generated sets of parameters was:

$$\theta_a = 0.7513, \;\; \theta_{ba} = 0.2551, \;\; \theta_{bc} = 0.6320, \;\; M_{cb} = 0.6991, \;\; M_{ca} = 3.6727. \tag{19}$$

The corresponding transition probabilities and each cycle probability are shown in Table 1 (nominal value column). The predicted transition cycle is $c8a$, which indeed corresponds to the observed periodic orbit.

To control the system towards a length 6 cycle, we have used Proposition 6.3. Since $P^{\text{two}}_{112} = 1$, and to guarantee that $M_{ca} > 1$, we choose $M_{cb} < \min\{\theta_{bc}, 0.95(1-1/(1+(B-1)/4)\}$, and next set $M_{ca} = 0.5+0.5(1-M_{cb})(1+(B-1)/4)$. To control the system towards a length 10 cycle, we have used Proposition 6.1, choosing $M_{cb} = 0.7+0.3\times 2\theta_{bc}/(1+\theta_{bc})$ This consists of increasing the contribution from the short negative feedback loop. Computing the new lower bound for M_{ca} shows that the nominal value for M_{ca} can be used. The new parameters and transition probabilities are given in Table 1. For both cases, the predicted transition cycle coincides with the observed periodic orbit, as can be seen by comparison of Table 1 and Fig. 8.

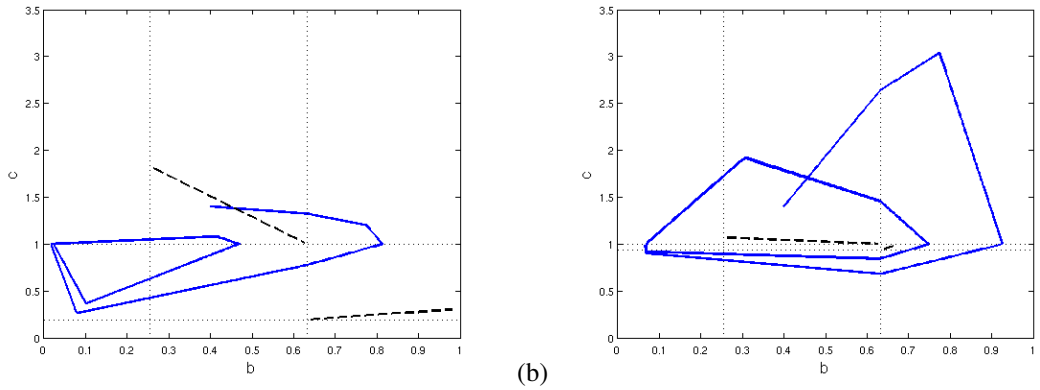

Figure 8: Controlling the system to a periodic orbit (solid line) that follows length 6 or length 10 transition cycles. Dashed lines represent separatrix curves. The figure shows the projection on the plane bc of the trajectory of system (10) with parameters (19), except: (a) $M_{cb} = 0.1937$ and $M_{ca} = 1.0064$, or (b) $M_{cb} = 0.9324$, $M_{ca} = 3.6727$.

7 Conclusions

Two definitions of transition probability have been introduced, that relate the parameters of piecewise affine systems with the qualitative dynamics in the corresponding transition graph. Among other applications, this approach can be used to estimate some of the parameters of the PWA system or predict which orbit is more likely to occur for a given set of parameters, in the case of systems with several possible transition cycles. The two definitions both depend on the volume of initial conditions that cross from the current domain to a neighbouring domain, but one of them also uses some memory of the trajectory: this memory provides an indication of impossible two-step transitions, which improves the prediction of the observed periodic orbit.

This study deals only with systems where there are at most two possible transitions from each hyperrectangle, which is a very limiting constraint. However, the generalization of the probabilities for multiple (> 2) transitions from a given domain will be hard for general PWA systems with distinct degradation rates and multiple thresholds for each variable. One possible step towards a generalization is to consider first the case of equal degradation rates, which highly simplifies the expressions of the probabilities (see Propositions 4.1 and 4.2 with $g_{ab} = g_{bc} = 1$). More generally, with equal degradation rates these probabilities are the volumes of polytopes. These polytopes have been explicitly described in terms of affine inequalities, for all possible configurations [7]. Even though the exact calculation of the volume of a general polytope is hard [2], it can be much easier for particular polytopes, like hypercubes, or simplices. Further work might thus extend the results of this paper to higher dimensions. Alternatively, if the parameters of the system are known, Monte-Carlo approaches using samples of points in a regular domain could be used to estimate the transition probabilities of a higher-dimensional system, see [25] for an example in a different context.

Nevertheless, an interesting outcome of this study is a method for finding sets of parameters that will lead the system to a given periodic orbit or, conversely, predicting which periodic orbit the system will most likely follow given a set of parameters. Even if this method gives only probabilistic answers, it is still valuable, as there are very few methods for studying the existence of periodic orbits in a general nonlinear system.

References

[1] Belta, C., Habets, L., Kumar, V.: Control of multi-affine systems on rectangles with applications to hybrid biomolecular networks. In: Proc. 41st IEEE Conf. Decision and Control (CDC02), vol. 1, pp. 534–539 (2002)

[2] Büeler, B., Enge, A., Fukuda, K.: Exact volume computation for convex polytopes: a practical study. In: G. Ziegler (ed.) PolytopesCombinatorics and Computation. Birkhuser, Basel (2000)

[3] Casey, R., de Jong, H., Gouzé, J.: Piecewise-linear models of genetic regulatory networks: equilibria and their stability. J. Math. Biol. **52**, 27–56 (2006)

[4] Chaves, M., Gouzé, J.: Exact control of genetic networks in a qualitative framework: the bistable switch example. Automat. **47**, 1105–1112 (2011)

[5] Chaves, M., Tournier, L., Gouzé, J.L.: Comparing Boolean and piecewise affine differential models for genetic networks. Acta Biotheor. **58**(2), 217–232 (2010)

[6] Edwards, R.: Analysis of continuous-time switching networks. Physica D **146**, 165–199 (2000)

[7] Farcot, E.: Geometric properties of a class of piecewise affine biological network models. J. Math. Biol. **52**(3), 373–418 (2006)

[8] Farcot, E., Gouzé, J.: A mathematical framework for the control of piecewise-affine models of gene networks. Automatica **44**(9), 2326–2332 (2008)

[9] Farcot, E., Gouzé, J.: Periodic solutions of piecewise affine gene network models with non uniform decay rates: the case of a negative feedback loop. Acta Biotheor. **57**, 429–455 (2009)

[10] Friedman, N.: Inferring cellular networks using probabilistic graphical models. Science **303**(5659), 799–805 (2004)

[11] Giannakopoulos, F., Pliete, K.: Planar systems of piecewise linear differential equations with a line of discontinuity. Nonlinearity **14**, 1611–1632 (2001)

[12] Glass, L.: Combinatorial and topological methods in nonlinear chemical kinetics. J. Chem. Phys. **63**, 1325–1335 (1975)

[13] Glass, L., Kauffman, S.: The logical analysis of continuous, nonlinear biochemical control networks. J. Theor. Biol. **39**, 103–129 (1973)

[14] Glass, L., Pasternak, J.: Stable oscillations in mathematical models of biological control systems. J. Math. Biol. **6**, 207–223 (1978)

[15] Gouzé, J., Chaves, M.: Piecewise affine models of regulatory genetic networks: review and probabilistic interpretation. In: J. Lévine, P. Müllhaupt (eds.) Advances in the Theory of Control, Signals and Systems, with Physical Modelling, *Lecture Notes in Control and Information Sciences*, vol. 470, pp. 241–253. Springer (2010)

[16] Gouzé, J., Sari, T.: A class of piecewise linear differential equations arising in biological models. Dyn. Syst. **17**(4), 299–316 (2002)

[17] Habets, L., Schuppen, J.v.: A control problem for affine dynamical systems on a full-dimensional polytope. Automatica **40**, 21–35 (2004)

[18] Hoffmann, A., Levchenko, A., Scott, M., Baltimore, D.: The IkB-NFkB signaling module: temporal control and selective gene activation. Science **298**, 1241–1245 (2002)

[19] Lee, I., Date, S., Adai, A., Marcotte, E.: A probabilistic functional network of yeast genes. Science **306**(5701), 1555–1558 (2004)

[20] Mestl, T., Lemay, C., Glass, L.: Chaos in high-dimensional neural and gene networks. Physica D **98**, 33–52 (1996)

[21] Shmulevich, I., Dougherty, E., Kim, S., Zhang, W.: Probabilistic Boolean networks: a rule-based uncertainty model for gene regulatory networks. Bioinformatics **18**(2), 261–274 (2002)

[22] Snoussi, E.: Qualitative dynamics of piecewise-linear differential equations: a discrete mapping approach. Dyn. Stab. Syst. **4**(34), 189207 (1989)

[23] Thomas, R., D'Ari, R.: Biological Feedback. CRC-Press, Boca Raton, Florida (1990)

[24] Tournier, L., Chaves, M.: Uncovering operational interactions in genetic networks using asynchronous boolean dynamics. J. Theor. Biol. **260**(2), 196–209 (2009)

[25] Wiback, S., Famili, I., Greenberg, H., Palsson, B.: Monte carlo sampling can be used to determine the size and shape of the steady-state flux space. J. Theor. Biol. **228**(4), 437–447 (2004)